A parametric study of the effect of arterial wall curvature on non-invasive assessment of stenosis severity: computational fluid dynamics study

Kalimuthu Govindaraju[1,*], Girish N. Viswanathan[2], Irfan Anjum Badruddin[3], Sarfaraz Kamangar[3], N. J. Salman Ahmed[4] and Abdullah A. A. A. Al-Rashed[5]

[1]Centre for Engineering Programs, HELP College of Arts and Technology, Kuala Lumpur, Malaysia
[2]Consultant Interventional Cardiologist, Derriford Hospital, Plymouth and Clinical Research Fellow, Newcastle University, Newcastle upon Tyne, United Kingdom
[3]Department of Mechanical Engineering, University of Malaya, Malaysia
[4]Centre for Energy Sciences, Department of Mechanical Engineering, University of Malaya, Kuala Lumpur, Malaysia
[5]Department of Automotive and Marine Engineering Technology, College of Technological Studies, The Public Authority for Applied Education and Training, Kuwait

The effect of coronary arterial wall curvature on non-invasive assessment of stenosis severity was studied by examining the fractional flow reserve (FFR), pressure drop coefficient (CDP) and lesion flow coefficient (LFC) under different angles of curvature of the arterial wall models. Computational simulation of hyperemic blood flow in curved arteries with different angles of curvature (0°, 30°, 60°, 90° and 120°) was developed in three severe categories of stenosis of 70% (moderate), 80% (intermediate), and 90% (severe) area stenoses (AS) to evaluate the effect of curvature on FFR, CDP and LFC. The numerical study showed that for a given percentage of AS, the curvature of the arterial wall augmented the flow resistance in addition to the resistance caused by the stenosis. Also, there are significant differences in FFR, CDP and LFC between a straight and a curved section. With an increase in artery wall curvature from 0° to 120°, FFR significantly decreases by 5%, 8% and 20% in 70%, 80% and 90% AS respectively. For a fixed stenosis severity, CDP significantly increases, whereas LFC decreases as the angle of curvature changes from straight to curved section. We conclude that the significant differences in FFR, CDP and LFC confirms that the functional significance of stenosis assessed non-invasively could lead to misjudgment of its severity. This will notably influence the intermediate stenosis severity. So the arterial wall curvature should be considered when assessing the significance of stenosis as an alternative to FFR.

Keywords: Blood flow, computational fluid dynamics, non-invasive assessment, stenosis severity, straight and curved arteries.

ATHEROSCLEROSIS is a chronic disease which involves the build-up of fatty deposits and cholesterol within the arterial wall, eventually leading to lumen narrowing, i.e. stenosis. This condition impairs blood flow to the heart muscle and results in life-threatening myocardial infarction[1]. Atherosclerotic plaque formation develops and progresses in the arterial branches, arterial bend segments, aortic T-junctions and artery bifurcations where the zones of complex spiral secondary flow and recirculation are formed[2,3]. The curvature or radius of curvature is defined as the degree of artery vessel deviation from being straight at a given point, which refers to the radius of a circle that mathematically best fits the curve at that point[2]. Thus, a coronary vessel with a small radius bends more sharply than a vessel with a large radius. From a macroscopic perspective, these vessels differ from each other in dimension and shape. Therefore, studies of functional significance of stenosis formed in the curved section of the artery are significant.

Assessing the functional significance of intermediate stenosis severity remains a challenge for cardiologists[4]. In the current clinical setting, fractional flow reserve (FFR; which is the ratio of the distal pressure to the aorta pressure under maximal hyperemia) is a clinically well-proven parameter for measuring the functional severity of stenosis[5]. Numerous clinical trials showed that stenoses with FFR < 0.75 benefit from coronary intervention in single-vessel coronary artery disease (CAD)[6], whereas stenoses with FFR > 0.8 are not associated with exercise-induced ischemia[5,7]. A cut-off value of 0.8 was used in FAME1 (fractional flow reserve versus angiography for multi-vessel evaluation 1) and FAME2 study[8], which is currently considered as the accepted standard for assessing hemodynamic significance in both single and

*For correspondence. (e-mail: govindarajuk@helpcat.edu.my)

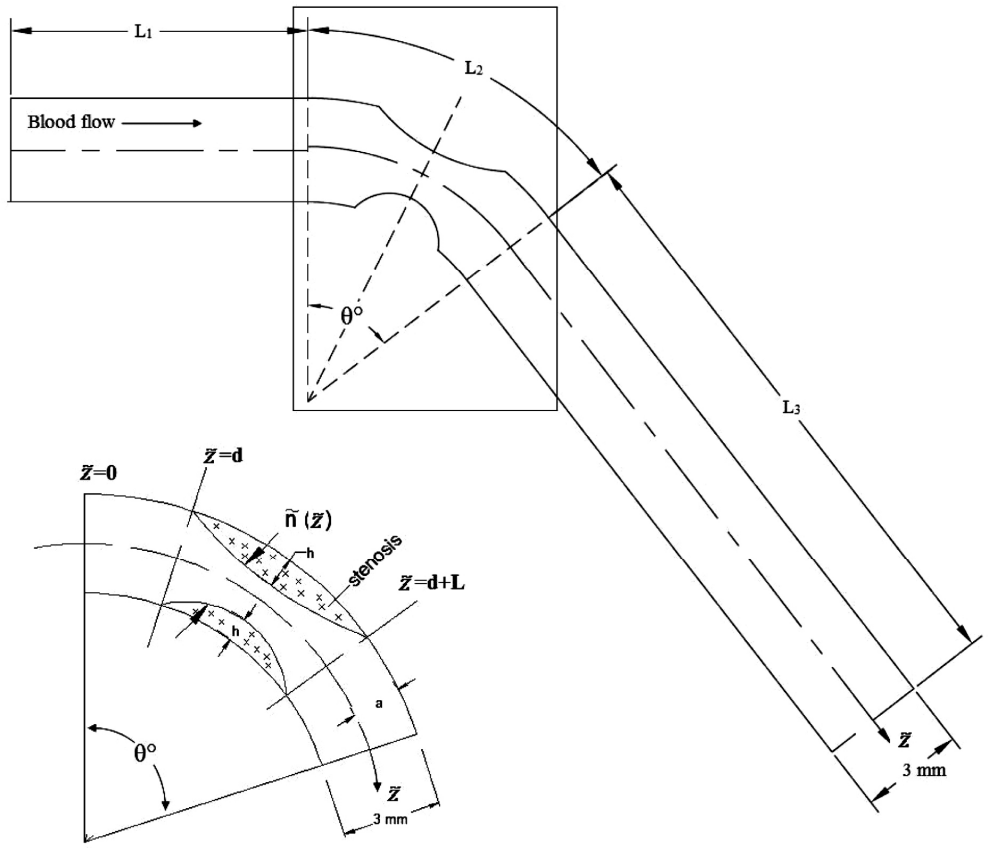

Figure 1. Schematic diagram of a curved artery with stenosis.

multi-vessel disease. The recently proposed futuristic parameters such as pressure drop coefficient (CDP) and lesion flow coefficient (LFC), which are derived from the basic fluid dynamic principles[9], are useful in diagnosing stenosis severity. Researchers have shown that CDP has a wide range of values for moderate, intermediate and severe stenosis[10] and LFC has a wider variability between the pre-percutaneous coronary intervention (PCI) and post-PCI groups in comparison with FFR[11]. So they can be used as a diagnostic index and thus, they have their own clinical importance.

Several experimental, analytical and computational simulation analyses conducted on the hemodynamic changes in stenotic arteries and computing the severity of stenosis have been reported by many researchers in an axisymmetric stenotic straight tube[10,12–14]. A limited number of studies focused on the influence of the curved stenosed arterial wall on physiological diagnostic parameters. Here, 3D computational models of 70%, 80% and 90% area stenoses (AS) in the curved arteries with different angles of curvature have been used for a comparative study on the physiological diagnostic parameters. It is expected that the geometry of the artery plays a substantial role in evaluating physiological significance of stenosis severity *in vitro* as an alternative to FFR.

Methods

Stenosis geometry

To examine the influence of artery wall curvature, we considered 70%, 80% and 90% AS (percentage AS = 100% × (reference lumen area – minimum lumen area)/ reference lumen area) artery models with different angles of curvature. Figure 1 shows a general geometrical form of an ideal model of the curved stenosed rigid artery. The internal diameter of the unobstructed lumen is 3 mm. The angles of curvature ($\theta°$) for the curved arteries are 0° (straight section), 30°, 60°, 90° and 120° (ref. 15). The geometry of the stenosis considered for the analysis is identical to that of the geometry described by Dash *et al.*[16]. It has been developed in a concentric method with length L and is given by

$$\frac{\tilde{\eta}(\tilde{z})}{a} = 1 - \frac{h}{a}\sin\pi\left(\frac{\tilde{z}-d}{L}\right), \quad d \le \tilde{z} \le d+L, \tag{1}$$

where $\tilde{\eta}(\tilde{z})$ is the radius of the lumen, a the radius of an unobstructed artery (1.5 mm), d the axial distance measured along the z axis ($\tilde{z}$) between the start of curvature and the start of stenosis at the bend, and h is the maximum

projection of the stenosis into the lumen. The throat diameters for 70%, 80% and 90% AS were 1.64, 1.34 and 0.94 mm respectively. Lesion length of $L = 10$ mm has been considered, which is a categorized cut-off length as a sensitive prediction index for a categorized cut-off FFR value of 0.75 (ref. 17). For all the curvature models, we assume appropriate fixed lengths $L_1 = 18$, $L_2 = 18$ and $L_3 = 60$ mm are the straight entrance length prior to the curve, the axial length of the curved section and straight distal length immediately after the curve respectively[14,18,19]. To provide complete assessment of the curvature effect on FFR, CDP and LFC, three different locations of stenosis such as central, proximal and distal positions at the bend have been taken into consideration.

Computational blood flow modelling

Blood flow through the coronary artery is assumed to be incompressible, unsteady and governed by the Navier–Stokes equation

$$\rho\left(\frac{\partial v}{\partial t} + v \cdot \nabla v\right) = \nabla \cdot \tau - \nabla P, \tag{2}$$

and the continuity equation for the incompressible flow is given by

$$\nabla \cdot v = 0, \tag{3}$$

where v is the three-dimensional velocity vector, t the time, ρ the blood density, P the pressure and τ is the stress tensor. In this study, blood is assumed to be non-Newtonian and follows the Carreau model[14], whereas blood viscosity μ is given in poise (P) as a function of the shear rate $\dot{\gamma}$ (s^{-1}) and expressed as

$$\mu = \mu_\infty + (\mu_0 - \mu_\infty)[1 + (\lambda\dot{\gamma})^2]^{(n-1)/2}, \tag{4}$$

where $\lambda = 3.313$ s; $n = 0.3568$, $\mu_0 = 0.56$ P, $\mu_\infty = 0.0345$ P, and blood density (ρ) is assumed as 1050 kg/m^3. A finite volume software CFX14.0 (ANSYS Inc.) was used for flow simulations.

Meshing and boundary conditions

Computational domains were initially meshed with the hexahedral elements as shown in Figure 2. The total number of elements ranged from 200,000 to 250,000 for the 70%, 80% and 90% AS models. In order to ensure that the 3D numerical analysis was realistic, digitized data of velocity $u(t)$ (Figure 3)[14,20] and stress-free boundary condition[21] were applied at the inlet and outlet respectively. No slip condition was applied at the arterial wall. The velocity profiles for 70%, 80% and 90% AS were obtained from the mean hyperemic flow rate ($\tilde{Q}$) of 175, 165 and 115 ml/min respectively[14,22]. The mean Reynolds number for 70%, 80% and 90% AS was 354, 333, and 232 at proximal ($2\tilde{Q}/\pi\nu a$) respectively, and 610, 747 and 742 at throat ($2\tilde{Q}/(\pi\nu(a-h))$) respectively. The kinematic viscosity ν was considered as 0.035 (ref. 23). Under these conditions of stenosis severity, the probability of shear layer instabilities occurring at a relatively low Reynolds number is high because of the possible disturbances in the cardiac pulse and irregularities in the plaque anatomy under hyperemic flow conditions[23,24]. A shear stress transport turbulence model of the k–ω model family was adopted for flow modelling because of its accuracy and robustness in overcoming the near-wall treatment errors for low Reynolds number turbulence flow[25]. The throat diameters for 70%, 80% and 90% AS were 1.64, 1.34 and 0.94 mm respectively.

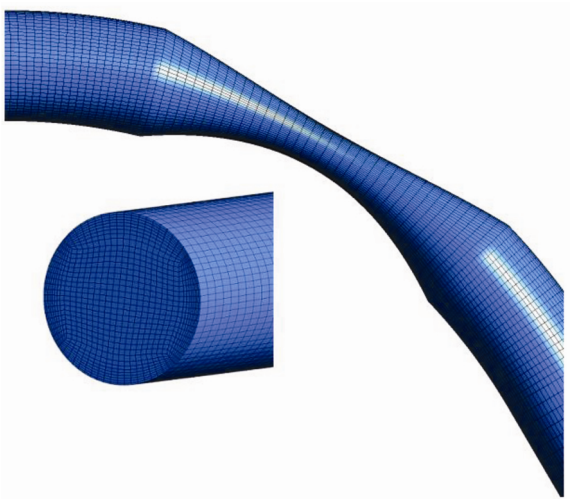

Figure 2. Computational mesh used for numerical study in the curved stenotic artery model.

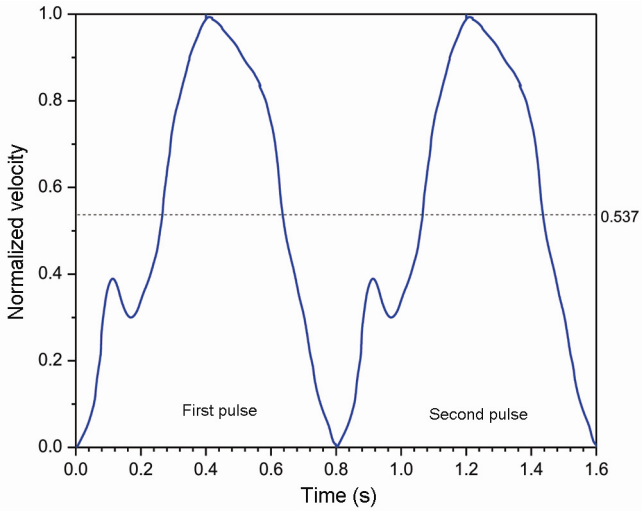

Figure 3. Physiological velocity applied at the inlet[14,20]. The peak velocity u_{p-t} corresponds to a normalized velocity of 1.0, so that the ratio of mean to peak velocity $\bar{u}/u_{p-i}$ is 0.537.

Numerical methodology

The CFD simulation was first run with steady-state flow analysis and then with transient flow analysis based on the results of the steady-state analysis as the initial estimate[25,26]. For the steady-state analysis, values of the following parameters were set at the inlet and outlet:

- Mean blood flow model velocity at the inlet ($\tilde{U}_a$): 0.413, 0.389, and 0.271 m/s corresponding to 70%, 80% and 90% AS.
- Stress-free boundary condition at the outlet.

Periodic flow was ensured by running the transient flow analysis for 320 time steps (0.01 s per time step and a maximum of 10 internal iterations were solved per time step). It represented four cycles (0.8 s each) of pulsatile flow with each time step converging to a residual target of 1×10^{-4}. Without-guide-wire condition was considered in all cases. Figure 4 shows a mesh sensitivity analysis graph for the straight artery model having 80% AS. In this model, three grid densities with elements 246,620, 290,345 and 334,728 were considered and simulated for finding the pressure drop across the stenosis. The difference in the pressure drop between the last two grid systems was 0.3%; so the last fine grid system in the flow domain was adopted for computation of FFR, CDP and LFC. Similarly, mesh sensitivity analysis was carried out for the rest of the models.

Pressure drop in curved arteries

In all the curvature models, the overall transient pressure drop $\Delta p = p_a - p_d$ was taken during the cardiac cycles 3 and 4 (where a_p and d_p are instantaneous pressures measured at 3 mm before the arterial wall begins to bend and at distal recovery region along the axis of the coronary artery respectively). No significant difference in pressure drop was found between the cycles 3 and 4 and the average results reported here are from third and fourth cycles. Figure 5 shows the overall transient pressure drop in 0° and 120° curvature wall models having 80% AS. Time-averaged pressure drop was calculated as $\Delta\tilde{p} = \tilde{p}_a - \tilde{p}_d$ (where $\tilde{p}_a$ and $\tilde{p}_d$ are time-averaged instantaneous pressures of $\tilde{p}_a$ and $\tilde{p}_d$ respectively).

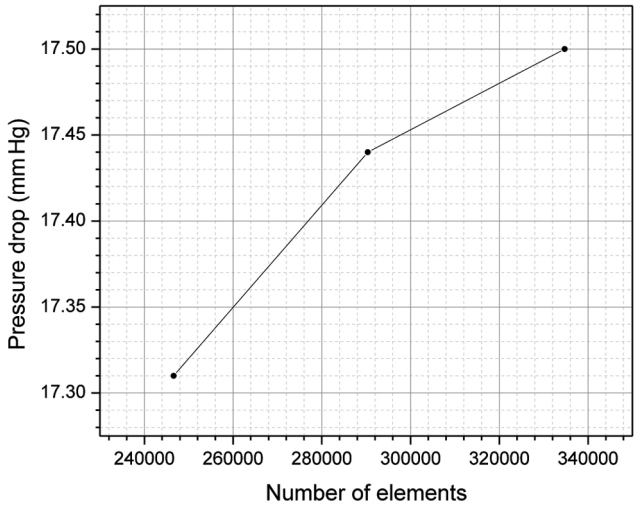

Figure 4. Mesh sensitivity analysis graph for the straight artery model having 80% area stenosis.

Diagnostic parameters

Fractional flow reserve: FFR is defined as the ratio of hyperemic flow in the stenotic artery to the maximum flow if the same artery had been normal. This flow ratio is also expressed as the ratio of the distal pressure to the aortic pressure[5,6]:

$$\mathrm{FFR} = \frac{\tilde{p}_d}{\tilde{p}_a}, \tag{5}$$

where $\tilde{p}_a$ is the time-averaged proximal stenotic pressure (mm Hg) and $\tilde{p}_d$ is the time-averaged distal stenotic pressure (mm Hg) measured when the end of flow reversal has occurred[14].

Pressure drop coefficient

At hyperemia, CDP is a dimensionless functional parameter derived from the principles of fluid dynamics by considering the time-averaged pressure drop ($\Delta\tilde{p}$) and velocity proximal to the stenosis[9,14].

$$\mathrm{CDP} = \frac{\Delta\tilde{p}}{0.5\rho\tilde{U}_a^2}, \tag{6}$$

where $\Delta\tilde{p} = (\tilde{p}_a - \tilde{p}_d)$ (N/m^2) and $\tilde{U}_a$ is the inlet proximal velocity of blood (m/s). CDP is associated with the viscous loss and loss due to momentum change in blood flow through the stenosis.

Lesion flow coefficient

Banerjee *et al.*[9] developed the normalized and non-dimensional functional diagnostic parameter LFC at hyperemia by considering the functional end-points and geometric parameters. LFC ranges from 0 to 1, and is the ratio of %AS and the square root of CDP evaluated at the stenosis site.

$$\mathrm{LFC} = \frac{\%AS}{\sqrt{\Delta\tilde{p}/0.5\rho\tilde{U}^2_{(a-h)}}},$$

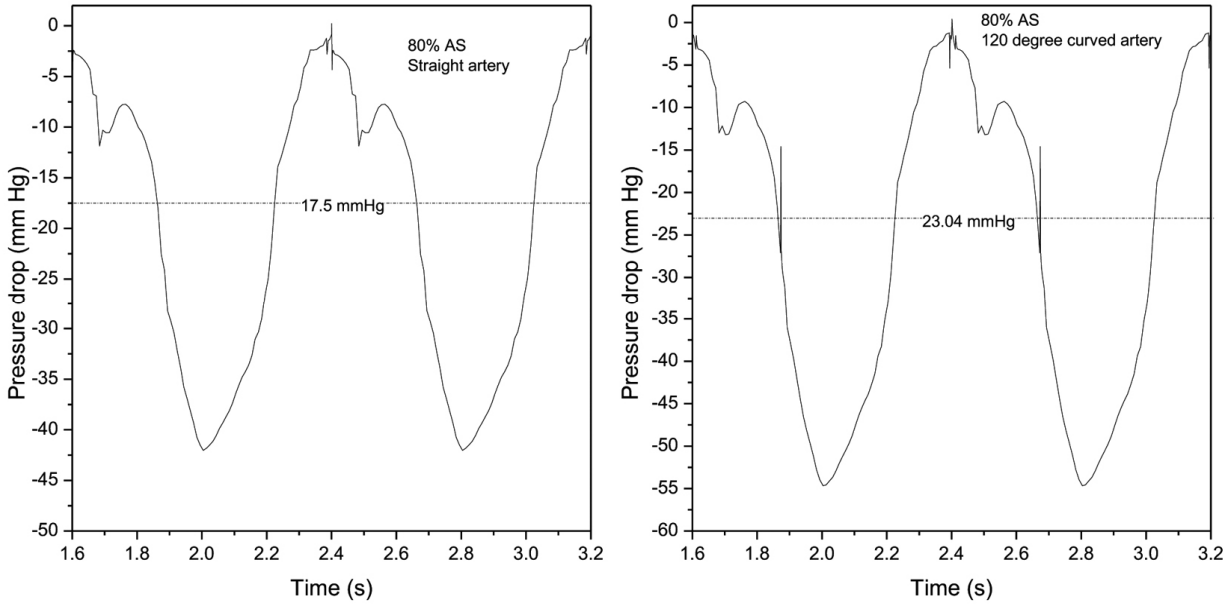

Figure 5. Overall transient pressure drop in straight and 120° stenosed curved artery having 80% AS.

where $\tilde{U}^2_{(a-h)}$ is the mean velocity of blood at the stenosis site (m/s).

Statistical analysis

Computed data were collected as continuous and categorical from the numerical study. The $\Delta\tilde{p}$, FFR, CDP and LFC values obtained from all the configurations were entered into SPSS 22.0 (SPSS, Inc, Chicago, IL, USA) for statistical analysis. A *P*-value of <0.05 was considered statistically significant. A one-way repeated measure ANOVA between groups with post-hoc comparison was used for analysis of computed data to determine the differences in the curvature.

Results

Comparison of diagnostic parameters

For a given %AS, there were significant differences in $\Delta\tilde{p}$, FFR, CDP and LFC between straight and curved artery models as tested with one-way repeated measure ANOVA ($P < 0.05$). The post-hoc test indicated that $\Delta\tilde{p}$, FFR, CDP and LFC between 30° and 60° ($P > 0.05$), 60° and 90° ($P > 0.05$), and 90° and 120° ($P > 0.05$) were not significant. However, these parameters in the remaining pairwise combinations of curvature were statistically significant ($P < 0.05$). There was no significant difference in $\Delta\tilde{p}$/FFR/CDP/LFC between stenosis location changed from upstream to central and central to downstream position at the bend for a given %AS and for a given angle of curvature. All computed $\Delta\tilde{p}$, FFR, CDP and LFC values reported in the following sections were obtained with the stenosis located centrally at the bend.

Effect of curvature on flow and pressure drop

Table 1 provides the computed $\Delta\tilde{p}$ across the stenosis in 70%, 80% and 90% AS for the various angles of curvature. For a given angle of curvature of the arterial wall, $\Delta\tilde{p}$ increases as %AS increases. There is also an additional increase in $\Delta\tilde{p}$ as the angle of curvature increases for a given %AS and this is significant (Figure 6 *a*).

As the angle of curvature changes from 0° to 120°, the corresponding $\Delta\tilde{p}$ increases from 8.09 to 11.98 mm Hg (48%), 17.5 to 23.04 mm Hg (32%), and 40.92 to 49.8 mm Hg (22%) in 70%, 80% and 90% AS respectively. This finding indicates that the presence of curvature elevates the flow resistance in addition to the resistance caused by the stenotic lesion. Therefore, the major pressure drop is due to the stenosis, which is higher at the region of the minimal area of cross-section and the curvature of the arterial wall contributes to additional pressure drop in the curved artery.

Effect of curvature on coronary diagnostic parameters

Effect of curvature on FFR: The computed FFR decreases as %AS increases. For a given %AS, FFR decreases significantly when the angle of curvature of the artery increases (Figure 6 *b*). As the angle of curvature changes from 0° to 120°, FFR decreases from 0.91 to 0.86 (5%), 0.8 to 0.74 (8%), and 0.54 to 0.43 (20%) in

Table 1. Effect of different angles of curvature on $\Delta\tilde{p}$, FFR, CDP and LFC

Angle of curvature (θ)	70% AS					80% AS					90% AS				
	$\tilde{p}_a$ (mm Hg)	$\Delta\tilde{p}$ (mm Hg)	FFR	CDP	LFC	$\tilde{p}_a$ (mm Hg)	$\Delta\tilde{p}$ (mm Hg)	FFR	CDP	LFC	$\tilde{p}_a$ (mm Hg)	$\Delta\tilde{p}$ (mm Hg)	FFR	CDP	LFC
0	87	8.09	0.91	12	0.67	87.04	17.5	0.8	29.4	0.74	88	40.92	0.54	141.5	0.77
30	87.28	10.12	0.88	15	0.60	87.35	20.79	0.76	34.9	0.68	88	44.71	0.49	154.6	0.74
60	87.13	10.8	0.88	16.1	0.58	87.31	22.18	0.75	37.2	0.66	88	47.35	0.46	163.7	0.72
90	87.29	11.35	0.87	16.9	0.57	87.27	22.69	0.74	38.1	0.65	88.02	47.88	0.46	165.6	0.71
120	86.79	11.98	0.86	17.8	0.55	87.11	23.04	0.74	39	0.64	87.99	49.8	0.43	172.2	0.70

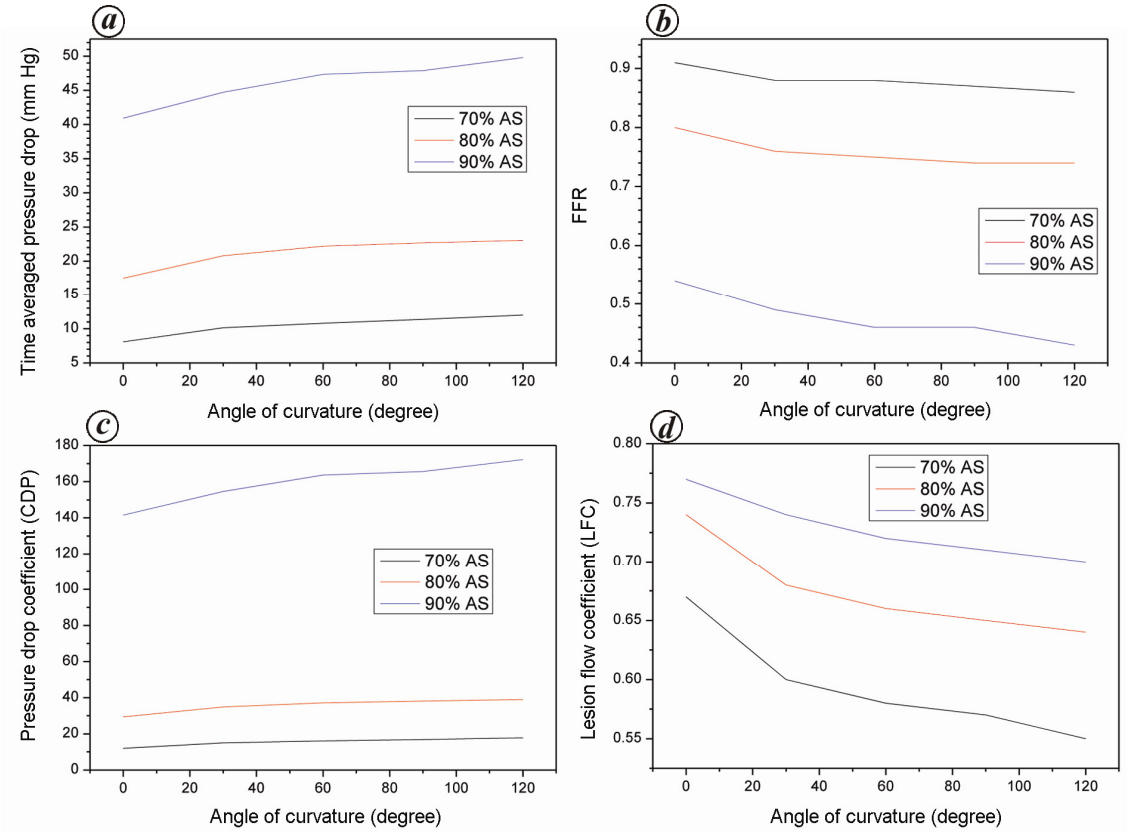

Figure 6. (***a***) Variation of time-averaged pressure drop across the stenosis in 70%, 80% and 90% AS for various angles of curvature. Variation of (***b***) fractional flow reserve (FFR). (***c***) Pressure drop coefficient (CDP) and (***d***) recession flow coefficient (LFC) with angle of curvature in 70%, 80% and 90% AS models.

70%, 80%, and 90% AS respectively. This finding indicates that the presence of curvature contributes to a decrease in FFR. A more significant effect is observed when the severity changes from intermediate to severe stenosis.

Effect of curvature on CDP and LFC: CDP and LFC are computed using the pressure, flow and lesion geometry in all the severity models. Figure 6 *c* and *d* shows the variation in CDP and LFC respectively, as the angle of curvature gradually varies from straight to a more curved section. For a given %AS, CDP increases from 12 to 17.8 (48%), 29.4 to 39 (33%), and 141.5 to 172.2 (22%) in 70%, 80% and 90% AS respectively, whereas LFC shows a decreasing trend as the angle of curvature of the arterial wall gradually varies from straight to a more curved section. LFC decreases from 0.67 to 0.55 (18%), 0.74 to 0.64 (14%), and 0.77 to 0.7 (9%) in 70%, 80% and 90% AS respectively.

Discussion

The primary objective of this work was to numerically examine the effect and consequences of angle of curvature of the stenosed arterial wall on FFR, CDP and LFC for a given %AS. This finding provides additional information about hemodynamic effect of stenosed curved

artery. Hence, it improves our understanding of *in vitro* assessment of stenosis severity as an alternate to FFR.

The $\Delta\tilde{p}$ value across the stenosis increases as %AS increases. This is due to the momentum changes caused by the increase in flow velocity across the stenosis configuration. Statistical analysis shows that for any fixed %AS, there is significant difference in $\Delta\tilde{p}$ and pressure-derived FFR values between straight and curved arteries. The axial flow velocity skewed caused by centrifugal pressure gradient associated with secondary flow, tends to push the flow in the curving plane toward the outer wall causing additional pressure drop in addition to the pressure drop due to area constriction (Figure 7), so $\Delta\tilde{p}$ in the curved vessels significantly increases with increase in the angle of curvature of the vessel. This finding is consistent with the results of Yao *et al.*[15]. The $\Delta\tilde{p}$ values obtained in the straight stenosed arteries (0° in curvature) with the rigid plaque models under all severity cases in this numerical study are in close agreement with those of Konala *et al.*[14] (Figure 8 *a*).

FFR derived from the pressure drop across the stenosis decreases as %AS increases and this finding is consistent with a previous *in vivo* study[27]. The present study reveals that the computed FFR value is significantly higher in the straight section of the stenotic coronary artery than in the 120° angle of the curvature stenotic models for a fixed %AS and flow. The FFR values obtained in the straight stenosed artery models for 70%, 80% and 90% AS in the rigid artery with the rigid plaque model (Figure 8 *b*) closely concur with the numerical results of Konala *et al.*[14]. Kristensen *et al.*[28] have reported a two-dimensional

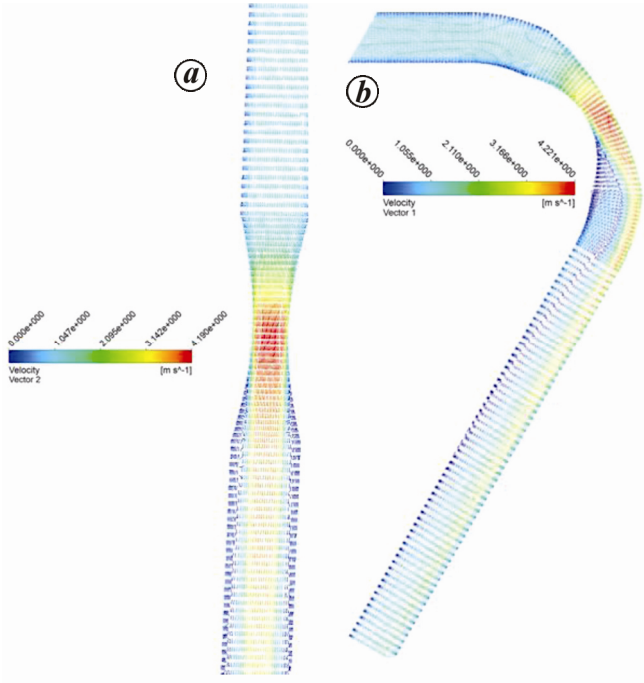

Figure 7. Without and with secondary flow in (***a***) straight and (***b***) curved artery models respectively.

plot of % AS versus FFR for individual hemodynamic clinical data, from which the FFR data around 70% AS were digitized and compared with those of the present study (Table 2). It is found that the numerical data in this study are in close agreement with the clinical data.

In the case of intermediate stenosis severity, the FFR values vary around the cut-off value of 0.75 owing to variations in hemodynamic conditions, which could lead to a dilemma for the clinician in distinguishing intermediate lesions that require stenting or simply need appropriate medical therapy. The FFR grey zone comprises a mere 5% difference (i.e. 0.75 to 0.80), which falls under intermediate stenosis severity. The present model confirms that any variation in the angle of curvature significantly affects $\Delta\tilde{p}$ and hence FFR for a given %AS. The threshold of FFR is determined in a large patient study; so curvature is already incorporated in this threshold. Nevertheless, measuring FFR in strongly curved arteries may lead to misjudgment (overestimate) of plaque severity and a correction may be applied when FFR values of 0.75–0.8 are obtained.

Numerically obtained CDP and LFC values in the straight sections of the artery models in this study were also compared with those of Konala *et al.*[14] (Figure 8 *c* and *d* respectively). Similar to FFR, CDP and LFC values vary with various angles of curvature in 70%, 80% and 90% AS (Figure 6 *c* and *d*). These are not clinically used as diagnostic parameters on their own, but are useful to get the complete picture of the functional significance of the stenosis severity in addition to FFR. However, for measuring these parameters, a combined flow/pressure wire is needed, while FFR needs only pressure wire. For clinical evaluation, the cut-off values for these parameters should be established, and related issues should be subjected to clinical research[29].

The results of this study support the idea that a single anatomic parameter such as percentage diameter stenosis/area stenosis is not equivalent to FFR for assessing functional significance of stenosis severity since the entire complex details of morphology of the geometry/stenosis play a role in FFR, measured by the pressure wire. Coronary computed tomography angiography (CCTA) has emerged as a non-invasive technique to evaluate the presence of coronary artery disease and non-invasive FFR derived from it, shows high diagnostic performance for the detection of ischemic stenosis[30,31]. From a clinical study by Kristensen *et al.*[28], %AS obtained from CCTA was found to be clinically useful and significantly correlated with FFR. Notably, the percentage difference between FFR of 0° and 120° curvature models was 7.5 in 80% AS (considered intermediate stenosis). This significant FFR variation caused by arterial wall curvature will notably affect the anatomical assessment of intermediate stenosis and it is probably near the region of diagnostic uncertainty. The effect of curvature should not be ignored when assessing stenosis severity by CCTA as an alternative

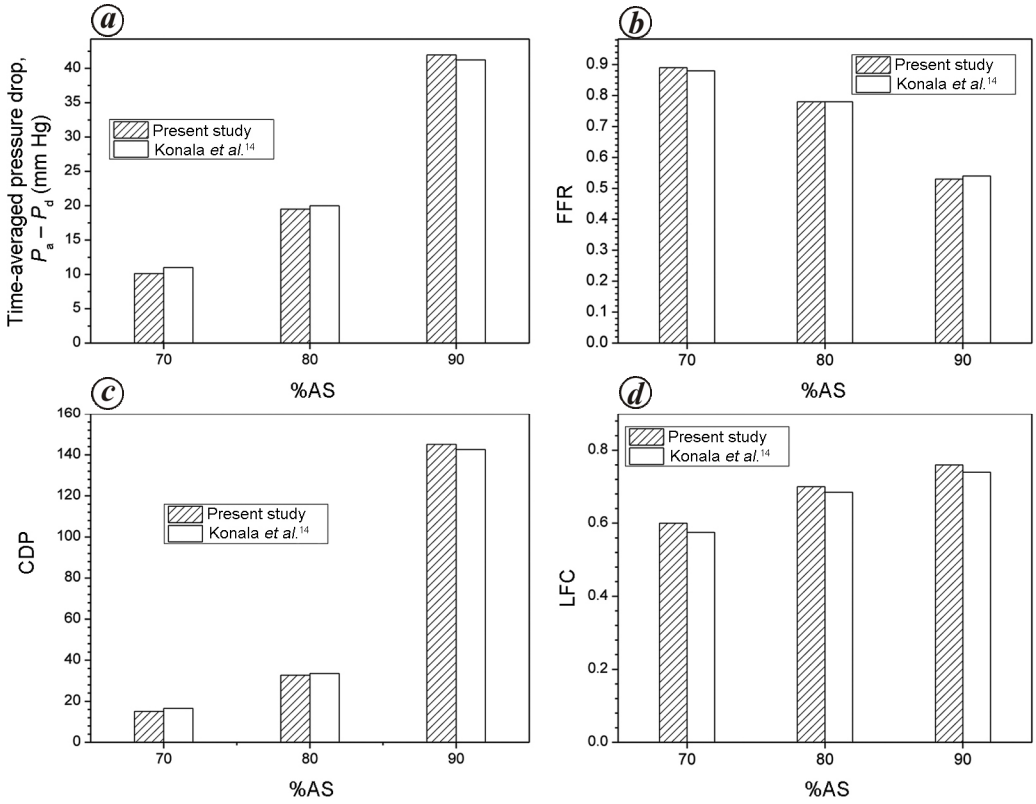

Figure 8. Comparison of numerically obtained $\Delta\tilde{p}$, FFR, CDP, LFC values with those of Konala *et al.*[14] in the straight section of stenotic coronary artery models for 70%, 80% and 90% AS.

Table 2. Comparison of clinical FFR data with the present numerical data

	Kristensen *et al.*[28] Percentage of area stenosis (% AS) measured around 70 with unknown angle of curvature	Present study 70% area stenosis Angle of curvature (θ)				
		0	30	60	90	120
FFR	0.86 (69.03% AS) 0.84 (70.08% AS) 0.89 (71.02% AS)	0.91	0.88	0.88	0.87	0.86

to FFR, despite the possibility that straight artery could result in FFR = 0.8.

The present study has significant limitations as well. Factors affecting the diagnostic parameters, such as arterial wall compliance[14], multiple bends, dynamic curvature variations due to heart motion[32], wall roughness, lesion eccentricity, diffused disease and tandem lesion have not been included in the study. Furthermore, in future studies, realistic coronary artery model need to be used, which will overcome the limitations to analyse the influence of artery wall curvature on anatomical assessment of stenosis severity.

Conclusion

This computational fluid dynamic simulation study has investigated the effects of angle of curvature on the coronary diagnostic parameters in 70%, 80% and 90% AS coronary artery models under hyperemic flow conditions. The results show that the changes in diagnostic parameters FFR, CDP and LFC from the straight to curved section of the artery model are significant for a given %AS. As the artery wall curvature varies from straight section to 120° curved section, the computed diagnostic parameter FFR decreases by 5%, 8% and 20% in 70%, 80% and 90% AS respectively. These variations in the diagnostic parameter confirm that the non-invasive assessment of stenosis leads to misjudgment of its severity. Aside from the plaque size, shape and its components, the curvature of the arterial wall influences the visual assessment of stenosis severity, particularly for the intermediate stenosis.

1. Naghavi, M. *et al.*, From vulnerable plaque to vulnerable patient: a call for new definitions and risk assessment strategies: Part II. *Circulation*, 2003, **108**, 1772–1778.

2. Wang, X. and Li, X., Biomechanical behaviors of curved artery with flexible wall: a numerical study using fluid–structure interaction method. *Comput. Biol. Med.*, 2011, **41**, 1014–1021.
3. Huang, R. F., Yang, T.-F. and Lan, Y.-K., Pulsatile flows and wall-shear stresses in models simulating normal and stenosed aortic arches. *Exp. Fluids*, 2010, **48**, 497–508.
4. Tobis, J., Azarbal, B. and Slavin, L., Assessment of intermediate severity coronary lesions in the catheterization laboratory. *J. Am. Coll. Cardiol.*, 2007, **49**, 839–848.
5. Pijls, N. H. J. and Sels, J.-W. E. M., Functional measurement of coronary stenosis. *J. Am. Coll. Cardiol*., 2012, **59**, 1045–1057.
6. Pijls, N. H., Van Gelder, B., Van der Voort, P., Peels, K, Bracke, F. A., Bonnier, H. J. and el Gamal, M. I., Fractional flow reserve. A useful index to evaluate the influence of an epicardial coronary stenosis on myocardial blood flow. *Circulation*, 1995, **92**, 3183–3193.
7. Tonino, P. A. L. *et al.*, Fractional flow reserve versus angiography for guiding percutaneous coronary intervention. *N. Engl. J. Med*., 2009, **360**, 213–224.
8. Melikian, N. *et al*., Fractional flow reserve and myocardial perfusion imaging in patients with angiographic multivessel coronary artery disease. *JACC: Cardiovasc. Interventions*, 2010, **3**, 307–314.
9. Banerjee, R. K., Sinha Roy, A., Back, L. H., Back, M. R., Khoury, S. F. and Millard, R. W., Characterizing momentum change and viscous loss of a hemodynamic endpoint in assessment of coronary lesions. *J. Biomechan*., 2007, **40**, 652–662.
10. Banerjee, R. K., Ashtekar, K. D., Helmy, T. A., Effat, M. A., Back, L. H. and Khoury, S. F., Hemodynamic diagnostics of epicardial coronary stenoses: *in-vitro* experimental and computational study. *BioMed. Eng. OnLine*, 2008, **7**, 1–22.
11. Peelukhana, S. V. *et al.*, Lesion flow coefficient: a combined anatomical and functional parameter for detection of coronary artery disease – a clinical study. *J. Invas. Cardiol*., 2015, **27**, 54–64.
12. Banerjee, R. K., Peelukhana, S. V. and Goswami, I., Influence of newly designed monorail pressure sensor catheter on coronary diagnostic parameters: A *in vitro* study. *J. Biomech.*, 2014, **47**, 617–624.
13. Sinha Roy, A., Back, L. H. and Banerjee, R. K., Guidewire flow obstruction effect on pressure drop-flow relationship in moderate coronary artery stenosis. *J. Biomech*., 2006, **39**, 853–864.
14. Konala, B. C., Das, A. and Banerjee, R. K., Influence of arterial wall-stenosis compliance on the coronary diagnostic parameters. *J. Biomech*., 2011, **44**, 842–847.
15. Yao, H., Ang, K. C., Yeo, J. H. and Sim, E. K., Computational modelling of blood flow through curved stenosed arteries. *J. Med. Eng. Technol*., 2000, **24**, 163–168.
16. Dash, R., Jayaraman, G. and Mehta, K., Flow in a catheterized curved artery with stenosis. *J. Biomech*., 1999, **32**, 49–61.
17. Brosh, D., Higano, S. T., Lennon, R. J., Holmes Jr., D. R. and Lerman, A., Effect of lesion length on fractional flow reserve in intermediate coronary lesions. *Am. Heart J*., 2005, **150**, 338–343.
18. Gross, M. F. and Friedman, M. H., Dynamics of coronary artery curvature obtained from biplane cineangiograms. *J. Biomech*., 1998, **31**, 479–484.
19. Kaazempur-Mofrad, M., Wada, S., Myers, J. and Ethier, C., Mass transport and fluid flow in stenotic arteries: axisymmetric and asymmetric models. *Int. J. Heat Mass Transfer*, 2005, **48**, 4510–4517.
20. Cho, Y. I., Back, L. H., Crawford, D. W. and Cuffel, R. F., Experimental study of pulsatile and steady flow through a smooth tube and an atherosclerotic coronary artery casting of man. *J. Biomech*., 1983, **16**, 933–946.
21. Govindaraju, K., Kamangar, S., Badruddin, I. A., Viswanathan, G. N., Badarudin, A. and Salman Ahmed, N. J., Effect of porous media of the stenosed artery wall to the coronary physiological diagnostic parameter: a computational fluid dynamic analysis. *Atherosclerosis*, 2014, **233**, 630–635.
22. Roy, A. S., Banerjee, R. K., Back, L. H., Back, M. R., Khoury, S. and Millard, R. W., Delineating the guide-wire flow obstruction effect in assessment of fractional flow reserve and coronary flow reserve measurements. *Am. J. Physiol. Heart. Circ. Physiol*., 2005, **289**, H392–H397.
23. Banerjee, R. K., Back, L. H., Back, M. R. and Cho, Y. I., Physiological flow analysis in significant human coronary artery stenoses. *Biorheology*, 2003, **40**, 451–476.
24. Mallinger, F. and Drikakis, D., Instability in three-dimensional, unsteady, stenotic flows. *Int. J. Heat Fluid Flow*, 2002, **23**, 657–663.
25. Jozwik, K. and Obidowski, D., Numerical simulations of the blood flow through vertebral arteries. *J. Biomech*., 2010, **43**, 177–185.
26. Kamangar, S., Kalimuthu, G., Anjum Badruddin, I., Badarudin, A., Salman Ahmed, N. J. and Khan, T. M. Y., Numerical investigation of the effect of stenosis geometry on the coronary diagnostic parameters. *Sci. World J.*, 2014, **2014**, 7.
27. Banerjee, R. K. *et al.*, Concurrent assessment of epicardial coronary artery stenosis and microvascular dysfunction using diagnostic endpoints derived from fundamental fluid dynamics principles. *J. Invas. Cardiol*., 2009, **21**, 511–517.
28. Kristensen, T. S., Engstrøm, T., Kelbæk, H., von der Recke, P., Nielsen, M. B. and Kofoed, K. F., Correlation between coronary computed tomographic angiography and fractional flow reserve. *Int. J. Cardiol.*, 2010, **144**, 200–205.
29. Peelukhana, S. V., Back, L. H. and Banerjee, R. K., Influence of coronary collateral flow on coronary diagnostic parameters: an *in vitro* study. *J. Biomech*., 2009, **42**, 2753–2759.
30. Taylor, C. A., Fonte, T. A. and Min, J. K., Computational fluid dynamics applied to cardiac computed tomography for noninvasive quantification of fractional flow reserve scientific basis. *J. Am. Coll. Cardiol*., 2013, **61**, 2233–2241.
31. Koo, B.-K. *et al.*, Diagnosis of ischemia-causing coronary stenoses by noninvasive fractional flow reserve computed from coronary computed tomographic angiograms: results from the prospective multicenter DISCOVER-FLOW (diagnosis of ischemia-causing stenoses obtained via noninvasive fractional flow reserve) study. *J. Am. Coll. Cardiol*., 2011, **58**, 1989–1997.
32. Yang, C. *et al.*, Cyclic bending contributes to high stress in a human coronary atherosclerotic plaque and rupture risk: *in vitro* experimental modeling and *ex vivo* MRI-based computational modeling approach. *Mol. Cell. Biomech*., 2008, **5**, 259.

ACKNOWLEDGEMENTS. We thank University of Malaya, Malaysia for funding the research under the grant number RP006A-13AET and PG212-2015B. We acknowledge the facilities provided by HELP College of Arts and Technology (HELP CAT), a member of the HELP Group. Thanks to Meenadevi Govidaraju for helping our research activities.

Received 30 April 2015; revised accepted 14 January 2016

doi: 10.18520/cs/v111/i3/483-491